Resonator spectrometer for precise broadband investigations of atmospheric absorption in discrete lines and water vapor related continuum in millimeter wave range

M. Yu. Tretyakov,[a] A. F. Krupnov, M. A. Koshelev, D. S. Makarov, E. A. Serov, and V. V. Parshin
Institute of Applied Physics, Russian Academy of Sciences, 46 Uljanova str., Nizhniy Novgorod 603950, Russia

(Received 8 January 2009; accepted 22 July 2009; published online 16 September 2009)

The instrument and methods for measuring spectral parameters of discrete atmospheric lines and water-related continuum absorption in the millimeter wave range are described. The instrument is based on measurements of the Fabry–Pérot resonance response width using fast phase continuous scanning of the frequency-synthesized radiation. The instrument allows measurement of gas absorptions at the cavity eigenfrequencies ranging from 45 to 370 GHz with the highest to date absorption variation sensitivity of 4×10^{-9} cm^{-1}. The use of a module of two rigidly bounded maximum identical resonators differing in length by exactly a factor of two allows accurate separation of the studied gas absorption and spectrometer baseline, in particular, the absorption by water adsorbed on the resonator elements. The module is placed in a chamber with temperature controlled between −30 and +60 °C, which permits investigation of temperature dependence of absorption. It is shown that systematic measurement error of discrete atmospheric line parameters does not exceed the statistical one and the achieved accuracy satisfies modern demands for the atmospheric remote sensing data retrieval. Potential systematic error arising from the neglect of the effect of water adsorption on mirror surfaces is discussed. Examples of studies of water and oxygen spectral line parameters as well as continuum absorption in wet nitrogen are given. © *2009 American Institute of Physics.* [doi:10.1063/1.3204447]

I. INTRODUCTION

Global monitoring of the Earth's atmosphere from satellite-, airplane-, and ground-based instruments in the millimeter and submillimeter (mm/submm) wave range requires development of absorption models providing retrieval of the atmospheric parameters from observational data. Such models must take into account, as most important inputs, parameters of resonant (or discrete) molecular absorption lines as well as nonresonant (or continuum) absorption. The majority of spectral parameters of the lines and the continuum is obtained in laboratory experiments. Accuracy of recovered atmospheric parameters depends directly on accuracy of laboratory measurements. Atmospheric parameters retrieval nowadays puts forth unprecedented requirements to the quality of spectroscopic parameters. In the work of Payan *et al.*[1] it is stated that "foreign-broadening parameters should be measured with an accuracy of 5% or better in order to avoid that systematic spectroscopic errors dominates the statistical retrieval error." In the review of Rothman *et al.*[2] it is even stated that "an accuracy better than 1% is now required for adequate retrievals for several species."

In spite of a large number of recent laboratory studies of mm/submm discrete atmospheric molecular line parameters (see, e.g., Ref. 3 and references therein), precise data on pressure broadening and shifting parameters of molecular spectral lines as well as their temperature dependences are still highly demanded. Some parameters of diagnostic atmospheric lines were never measured in laboratory, so theoretically calculated values of the parameters are used in the propagation models. Some other parameters were measured just once; therefore in view of possible systematic uncertainties (which are usually unknown and may exceed considerably the statistical error of measurement estimated by the authors), parameter values have to be validated by some other technique, preferably differing by the principle of operation.

Most uncertain is parameterization of continuum absorption, in particular, the water vapor related continuum. The uncertainty is related to the yet unknown physical original of the continuum, its weakness in comparison with absorption in regular discrete atmospheric molecular lines, and general difficulties of the water-related measurements. Under these conditions, the need to develop an instrument capable of increasing the accuracy of discrete line parameters as well as continuum absorption measurements becomes evident. A significant step in this direction was made in 2000 when we developed a resonator spectrometer with backward wave oscillator (BWO) fast lock-in system permitting precise digital frequency scanning in phase continuous regime.[4] This improvement provided the highest to the present moment absorption variation sensitivity of 4×10^{-9} cm^{-1}, which ensured high accuracy of discrete line parameter mea-

[a]Author to whom correspondence should be addressed. Electronic mail: trt@appl.sci-nnov.ru.

surements. Exclusion of the apparatus function ("baseline") and continuum absorption measurements problems was still not solved fully at this early stage of the spectrometer development. Meanwhile other studies directed toward the continuum absorption measurements went on. There were several measurements of the continuum absorption at a few discrete frequencies (see, e.g., Ref. 5–7 and references therein). Two recent broadband studies of the continuum should also be mentioned. The first one was undertaken by Podobedov *et al.*[8–10] who used a commercial Fourier transform spectrometer with multipass gas cell that allowed investigation of the water-related continuum in atmospheric transparency windows throughout the submm wave range (0.3–2.7 THz). The second work was performed by Meshkov and De Lucia[11,12] with the use of the millimeter wave cavity ringdown spectrometer operating in the 170–260 GHz range. In an earlier publication[11] the authors demonstrated applicability of their instrument for studying different parts of the continuum, including the one related to collisions of water molecules with other atmospheric gas species. However, in the subsequent publication[12] only dry air continuum components were investigated quantitatively; that study is irrelevant to the current paper. Broadband (100–210 GHz) measurement of the water-related continuum by the resonator spectrometer[13] also revealed strong influence of water adsorbing on resonator mirrors on results of the continuum parameters. Analysis of the millimeter/submillimeter wave range continuum measurement methods used in the earlier studies leads us to the conclusion that adsorbing of water molecules onto mirrors was a common factor capable of influencing the continuum parameters in humid gases obtained in all well-known laboratory experiments.[7–12,14] In all these cases gas cells with multiple reflections of radiation off inner mirrors (either resonator cell[7,11,12,14] or multipass cell[8,9]) were used as the most appropriate technique for investigation of the weak continuum absorption, although the problem of separation of water vapor absorption and absorption by water adsorbed on mirrors was not solved in the experiments.

To overcome the problem it was proposed to use the cavity length variation method,[13] which permits separation of these two types of absorption. The potential of the method was for the first time demonstrated in an earlier work.[4] It was shown that measurement of quality factors of the Fabry-Perot (FP) cavity using two or more different resonant lengths of the cavity at the same radiation frequency allows accurate determination of the radiation absorption by the gas filling the cavity. For completeness of the review, it should be mentioned that the authors in Refs. 11 and 12 were also studying the cavity length variation method in their setup.[15]

In the present paper we present a modified precise broadband resonator spectrometer for investigation of discrete atmospheric line parameters as well as for continuum absorption studies with a proven method of apparatus function exclusion, in particular, with separation of wet gas absorption and absorption due to water adsorbed on the cavity elements by the cavity length variation method.

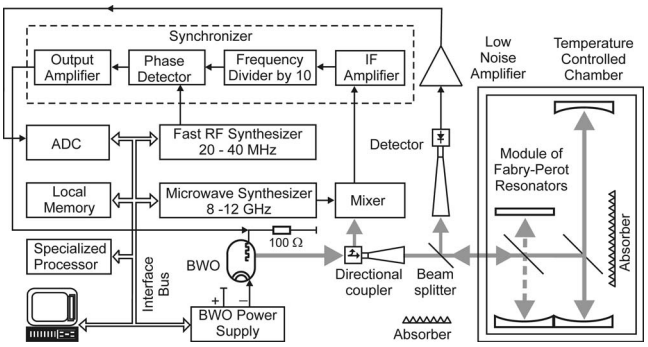

FIG. 1. Block-diagram of the resonator spectrometer.

II. TECHNICAL DETAILS OF THE SPECTROMETER

The first version of the resonator spectrometer and its main features were described in detail in Ref. 4. Later its capabilities were improved by developing the method of accounting for its baseline and small variations in temperature, pressure, and humidity of studied samples in the course of measurements[16] and by extending its operating frequency range up to 370 GHz.[17] Further evolution was the development of the temperature controlled chamber that allowed gas absorption investigations in the range from −30 up to +60 °C with temperature stability of about 0.2 °C.[18] In the present paper a method for eliminating systematic error caused by water molecules adsorbed on the resonator elements is proposed.

A block-diagram of the spectrometer is presented in Fig. 1. The principle of determining absorption is based on precise measurement of the Q-factor of the FP cavity. It is realized by fast recording of its resonance response during linear scan of exciting radiation frequency and subsequent determination of the response width by fitting its shape model function to the observed profile. The radiation source of the spectrometer is based on a BWO tube[19] whose radiation frequency is phase locked against a harmonic of the microwave (MW) synthesizer (Agilent E8257D). Scanning of the phase locked source frequency is performed by scanning the frequency of the phase detector reference signal. Use of the 20–40 MHz direct digital synthesizer (AD9850) output as the reference signal allows fast digital step-by-step frequency scan of the BWO within 200 MHz around the resonance response frequency. The most important property is that such a system provides a phase continuous frequency scan. Phase continuous excitation of the resonator permits avoiding long transitory processes during the frequency change and, in principle, allows reduction in the time necessary to record the FP cavity response down to $\sim 10\tau$ (τ is the time constant of the FP cavity) without loss of accuracy of determining its width.[20]

In the described setup the time of the resonator response recording (100 frequency steps) is limited to 6 ms due to the technical imperfections (low speed of the control processor used). Nevertheless, this time is short enough to eliminate the influence of low frequency noise distorting the shape of the response. The influence of other factors shifting the resonator response central frequency during the record (e.g., thermal drift) is eliminated by back and forth radiation frequency

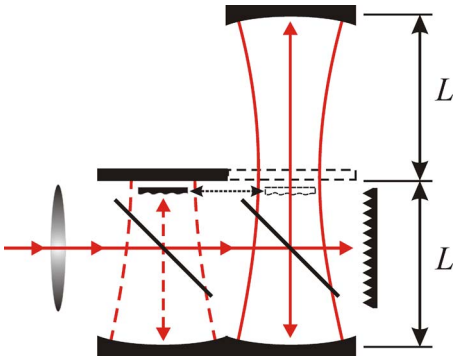

FIG. 2. (Color online) Direction of radiation beams and field distribution (not to scale) inside the module of double FP cavity. The position of the blocking switch corresponding to excitation of the long resonator is shown. The position of the temporarily used second flat mirror is shown by dashed rectangle.

scans and averaging of resulting resonance widths. This method, namely, fast precise back and forth phase continuous scans of synthesized radiation frequency and averaging of the recorded response width, is the key peculiarity of the spectrometer that allowed achievement of the record sensitivity to absorption variation of 4×10^{-9} cm^{-1} exceeding the sensitivity of available analogs by about one order of magnitude.[4] The studied absorption profile record consists of a set of absorption values at the known frequency points corresponding to eigenfrequencies of the FP cavity of fixed length. The fixed frequency interval between the points is within 0.2–0.4 GHz, depending on the particular cavity length used in the experiment. Tuning from one eigenfrequency of the FP cavity to another occurs automatically when the frequency of the MW synthesizer is changed.

The aforementioned method of cavity length variation is realized in the spectrometer using a module of double FP cavity consisting of two rigidly bounded maximum identical resonators differing in length by exactly a factor of two. The length of the longer resonator is limited by the size of the temperature controlled chamber and is 699.48 mm. Special efforts were undertaken to obtain maximum identical distribution of electric fields inside both of the resonators, as shown in Fig. 2. A spherical Teflon lens is used to correct a small divergence of the exciting radiation beam. Lower concave mirrors of both cavities are placed on the same solid plate at the bottom of the module. The upper concave mirror of the long cavity is fixed on a similar plate on top of the module, and the upper mirror of the short cavity is plane and is fixed on the third solid plate in the center of the module. All the three plates are connected to each other by six solid rods made of invar alloy. A special mount was designed for the plane mirror in order to compensate different thermal expansions of rods and mirrors, so the ratio of the long to the short cavity lengths was always equal to two, independent of the module temperature. All cavity mirrors (three spherical concave and one plane mirror) were made of hard brass, then optically polished and coated by silver. The mirrors were manufactured at once using the same technology and the same raw materials. Identity of reflection coefficient of the concave mirrors was checked by measurement of the response width of an open FP cavity having one reference mirror and one of the three new mirrors. The measurement was repeated with all three new mirrors changed one by one. The measured resonance widths differed from each other within a few percent, which could be considered as satisfactory agreement. Coupling elements for both cavities were made of one 5 μm thick polyethylene terephthalate film sheet (both film frames had the same orientation relative to the sheet) and were placed at 45° to the cavity axes at the same distance from the lower mirrors. An electromechanical switch blocks the electromagnetic field in one resonator and at the same time opens the other one. Thus, the excitation and the response recording for both resonators occur alternately.

The total fractional radiation intensity loss per one pass for each resonator in the module can be expressed through its constituents as

$$P_{\text{total}} = P_{\text{coupling}} + P_{\text{reflection}} + P_{\text{diffraction}} + P_{\text{gas}} = P_{\text{resonator}} + P_{\text{gas}}. \quad (1)$$

At the same time, it is known that the total loss can be determined from the resonator response full width at half maximum Δf (FWHM) as

$$P_{\text{total}} = \frac{2\pi L}{c}\Delta f, \quad (2)$$

where L is resonator length and c is light velocity in the substance.

The gas loss term from Eq. (1) can be expressed as

$$P_{\text{gas}} = 1 - e^{-\alpha l}, \quad \text{or} \quad P_{\text{gas}} = \alpha L \quad (3)$$

in the case of a small optical depth ($\alpha L \ll 1$), where α is gas absorption coefficient.

Since changes in the resonator losses due to a change in the gas index of refraction are negligibly small, the resonator loss $P_{\text{resonator}}$ can be found from its response width Δf_0 if the resonator is evacuated or filled with nonabsorbing gas,

$$P_{\text{resonator}} = \frac{2\pi L}{c}\Delta f_0. \quad (4)$$

By combining Eqs. (1)–(4), one can obtain a simple expression for the gas absorption coefficient,

$$\alpha = \frac{2\pi}{c}(\Delta f - \Delta f_0). \quad (5)$$

However, Eqs. (4) and (5) can be used in the case of dry gas investigations only. Due to adsorption of water molecules on mirror surfaces, reflection loss becomes a function of gas humidity and can be expressed as a sum of humidity-independent reflection loss of the empty or dry resonator loss and additional reflection loss,

$$P_{\text{reflection}} = P^{\text{dry}}_{\text{reflection}} + P^{\text{wet}}_{\text{reflection}}. \quad (6)$$

The assumption that these additional reflection losses are the same in both resonators of the module if no humidity and/or temperature gradients are present seems to be reasonable because of identical technologies of mirror manufacturing. Then the expression for the gas absorption coefficient can be easily derived from Eqs. (1)–(4) and (6) written for each

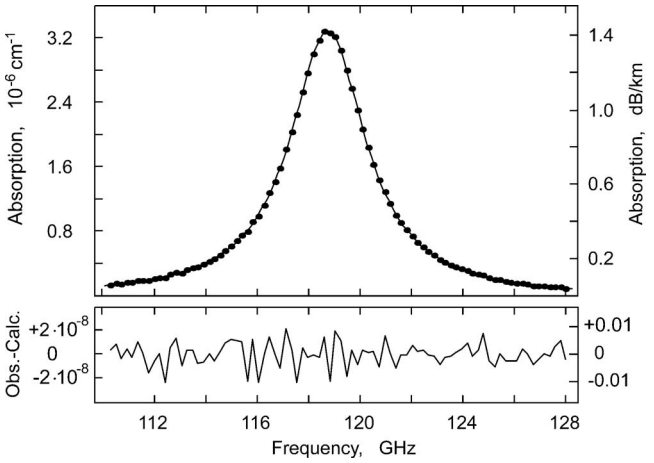

FIG. 3. Absorption profile of dry atmospheric air at 2.5 °C and 752 mm Hg in the vicinity of $N=1-$ transition of oxygen molecule recorded by means of the long resonator of the module. Experimentally measured absorption is shown by points. The solid line corresponds to the theoretical absorption profile fitted to the experiment. Residual of the fit is shown below to a larger scale.

resonator of the module, taking into consideration their length ratio ($L_2=2L_1=2L$),

$$\alpha = \frac{2\pi}{c}[2(\Delta f2 - \Delta f2_0) - (\Delta f1 - \Delta f1_0)], \tag{7}$$

where "1" and "2" correspond to the short and long resonators, respectively.

It should be emphasized that, in principle, the length variation method allows measuring the gas absorption coefficient with arbitrary L_1 to L_2 ratio. However, only exact doubling of the short cavity length, as shown in Fig. 2, allows accurate and convenient measurements because of fulfillment of the following necessary conditions: (i) maximum coincidence of the eigenfrequencies of the cavities, (ii) identical configuration of electromagnetic fields inside the cavities, and (iii) identical coupling conditions. In other cases there are more factors that may introduce systematic error into measurement results.

III. EXPERIMENTAL TESTS

A. Discrete molecular lines

An example of a discrete molecular absorption line record is given in Fig. 3. The line was recorded using only the long resonator of the module in the course of experimental cycle.[18] The value of the absorption was found using Eq. (5). For determination of Δf_0 (the resonator baseline), we used nitrogen having negligible absorption in this frequency range and ignored the small eigenfrequency detuning related to slightly different refraction indices of gases. The residual of the Rosenkranz's profile[21] fitted to the line record is shown in a magnified scale in the lower part of Fig. 3. Standard deviation of the residual points is 9×10^{-9} cm^{-1}. This value is in a very good agreement with the spectrometer absorption variation sensitivity of 4×10^{-9} cm^{-1} claimed in Ref. 4. The error is doubled because of the contribution of the spectrometer baseline [Eq. (5)] taken from the experiment. The signal-to-noise ratio of the record of this weak

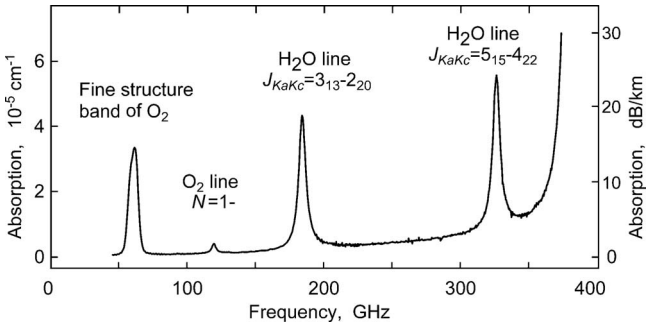

FIG. 4. Experimental record of laboratory atmosphere absorption spectrum in the 45–370 GHz range.

atmospheric line is about 340. This ensures a high statistical accuracy of the line spectroscopic parameters determined from the fit (see Ref. 18 for details). Discussion of possible systematic error of measurements by the spectrometer will be given below.

It should be mentioned that the spectrometer allows accurate determination of the following parameters of discrete molecular lines: (i) self- and foreign-gas pressure broadening and shifting,[16,22] (ii) mixing or collisional coupling,[23,24] (iii) integrated intensity,[16,22] and (iv) their temperature dependences.[18]

B. Broadband spectra

The experimental record of laboratory atmosphere absorption profile in the 45–370 GHz range at atmospheric pressure (730 Torr), room temperature (296 K), and usual ambient humidity (5.3 g/m^3) is presented in Fig. 4. As far as we know, this is the most broadband continuous millimeter wave atmosphere absorption spectrum recorded by one instrument to date. The absorption profile was recorded using only one resonator.[17] The record consists of five subranges corresponding to five different types of BWO used.

C. The continuum measurement related tests

The $N=1-$ oxygen line near 118.75 GHz in dry pure oxygen was used in the special test aiming at experimental verification of the aforementioned differential absorption measurement method [Eq. (7)] using both cavities of the module. The oxygen absorption coefficient at eigenfrequencies of each resonator in the module can be measured using Eq. (5). At the same time, absorption at eigenfrequencies of the short resonator (coinciding in the module described with those of the long one within the width of resonance response) can be determined using Eq. (7). Results of these three measurements are presented in Fig. 5 together with the absorption profile calculated by the millimeter wave propagation model.[23] All the results coincide within statistical experimental error.

The goal of the next test was to check similarity of $P^{\text{wet}}_{\text{reflection}}$ in two resonators of the module. For the test both resonators of the module were made identical by inserting the second plane mirror in the center of the long resonator, as shown by the dashed rectangle in Fig. 2. The mirror was manufactured together with all the other mirrors of the module. Then the chamber containing the module was filled with

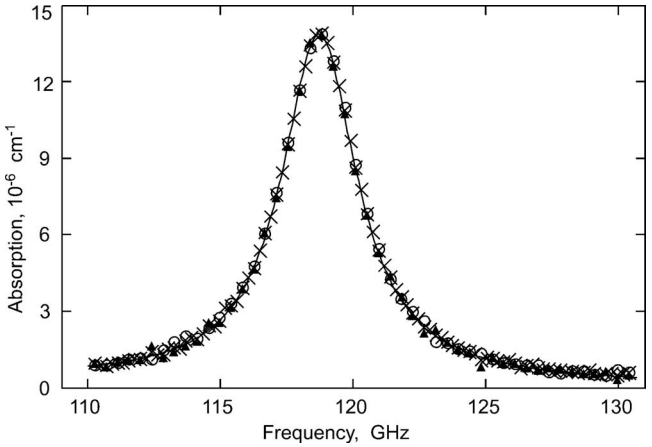

FIG. 5. Absorption profile of the $N=1-$ oxygen line measured by (i) long resonator (crosses), (ii) short resonator (empty circles), and (iii) "differential method" (filled triangles). Solid line corresponds to absorption profile calculated using MPM.

nitrogen, and resonance widths of each resonator at their eigenmodes at 130.36 GHz were measured varying nitrogen humidity stepwise from 0% up to 55% of relative humidity (RH). The experiment was repeated three times at temperatures of 7.5, 25.7, and 32.2 °C inside the chamber. The resulting dependences of the resonance width broadening $(\Delta f - \Delta f_0)$ versus humidity for each resonator are shown in Fig. 6.

We again expected coincidence of the dependences within statistical error. Nevertheless, a minor systematic discrepancy was found. It should be pointed out that the statistical spread of the experimental points is really small. Standard deviations of the points from the fitted second order polynomials (shown in Fig. 6 by solid lines) constitute only 44, 42, 35, 21, 12, and 15 Hz, respectively, from the upper to the lower trace. In terms of the absorption coefficient [Eq. (5)], this corresponds to an uncertainty of $(2.5-9) \times 10^{-9}$ cm^{-1}. The systematic discrepancy between the corresponding traces at high humidity is larger by about one order of magnitude. This is still quite a small value in terms of absorption. Nevertheless, a series of additional experiments was carried out, which revealed that the gas humidity affects not only the mirror reflection loss but also the coupling loss. (Results of this study will be published elsewhere.) By analogy with reflection loss $P^{\text{wet}}_{\text{reflection}}$, only the difference between additional water-related coupling losses of two resonators $(P2^{\text{wet}}_{\text{coupling}} - P1^{\text{wet}}_{\text{coupling}})$ would contribute to the aforementioned discrepancy observed in Fig. 6. Small difference in coupling losses of two resonators of the module in dry conditions $(P2^{\text{dry}}_{\text{coupling}} - P1^{\text{dry}}_{\text{coupling}})$ would not lead to the observed discrepancy because the difference is cancelled with baseline subtraction. If the angles between the resonator axis and the coupling film plane (coupling angles) are equal in both cavities and the coupling films are identical, then uniform adsorption of water molecules on the films should lead to the same change in dielectric constant of both films and, therefore, to the same change in coupling loss in both cavities. On the contrary, if coupling angles are different, the additional water-related coupling losses are also different and this can be a reason for the divergence of traces in Fig. 6. To confirm the difference in angles, the data of the experiment illustrated in Fig. 6 were revised, and the difference $[(f2-f2_0)-(f1-f1_0)]$ between the eigenfrequency shift in the resonators (f_0 and f are frequencies of the eigenmode of the resonator filled with dry and humid nitrogen, respectively) was analyzed. Mathematical equations related to the dependence of resonance width and shift on coupling angle, coupling film thickness, and dielectric constant are given, e.g., in Ref. 25. The analysis revealed the expected correspondence between the difference in the resonance frequency shifts and the difference in the resonance width broadenings within experimental error. This confirmed that these discrepancies between the traces observed in Fig. 6 originated from slightly different values of the coupling angles in this experiment. Small detuning of the coupling film angles from the initial 45° occurred as the result of manual optimization of the resonator response amplitudes in the course of preparing the experiment. Just for demonstration of the angle effect contribution, it is worth mentioning that in the configuration of the described resonators and for dielectric constant of the coupling film of three (the polyethylene terephthalate film passport claims $\varepsilon=3.0$ at 1 MHz), a change in the coupling angle by 2° only would compensate the discrepancy observed in Fig. 6 at maximum humidity. Thorough alignment of the coupling of the module with exciting radiation was undertaken, making sure that both coupling films were at the same distance from the lower mirrors and the coupling angles were exactly 45°. To increase the accuracy of the alignment, the BWO was temporally disconnected from spectrometer feeding waveguides and replaced by a He–Ne laser so that its beam shined through the whole system and controlled coincidence of the laser light reflection dots at the cavity mirrors. After the alignment the divergence of traces (Fig. 6) was eliminated.

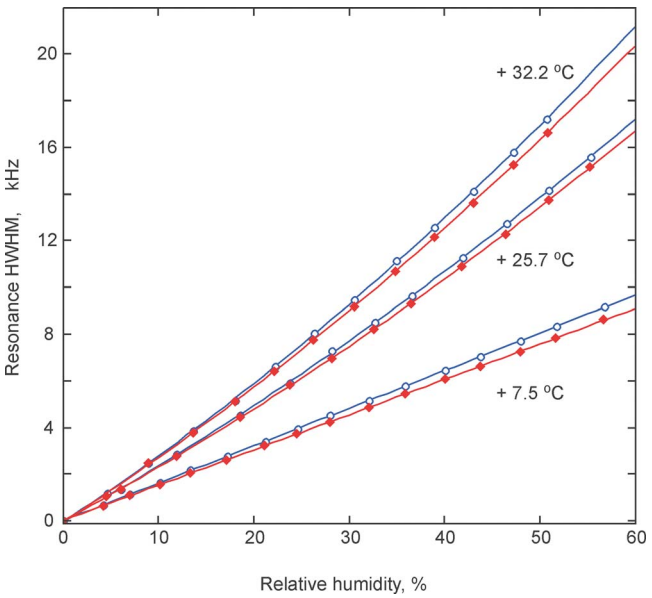

FIG. 6. (Color online) Resonance width broadening vs. nitrogen humidity for two identical resonators of the module at three different temperatures. Data of one resonator are shown by empty circles and of the other one by diamonds. The solid lines are quadratic polynomials fitted to the corresponding data.

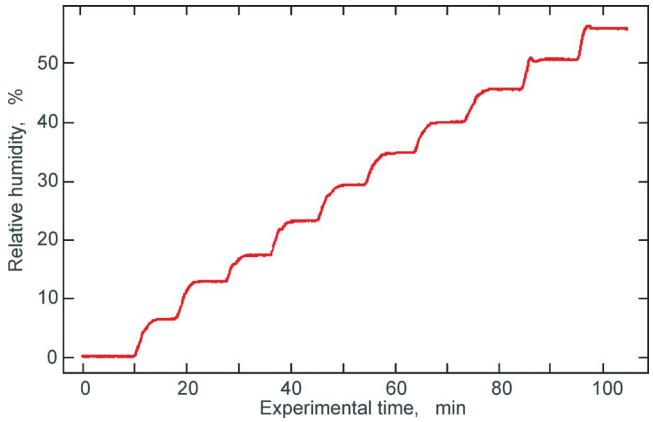

FIG. 7. (Color online) Typical dependence of humidity inside spectrometer chamber vs time of experiment during water-related continuum studies.

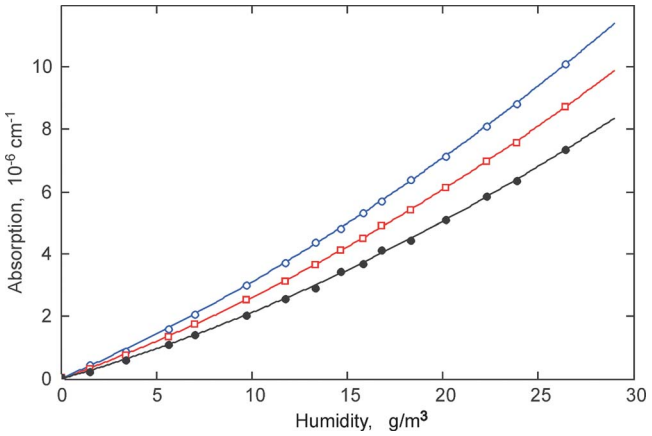

FIG. 8. (Color online) Absorption coefficient of humid nitrogen at 130.38 GHz, 747 mm Hg, and 40 °C measured by the short cavity (empty circles), by the long cavity (empty squares), and by the differential method (filled circles). The solid lines are second order polynomials fitted to points.

Thus, the experiment with identical resonators in the module proved, to an accuracy of the experiment, the assumption about similar change in the mirrors' reflectivity in the two resonators with the change in gas humidity. The experiment also revealed an unexpected dependence of the coupling loss on humidity, which, to the best of our knowledge, has not been mentioned and studied before, although it could also be a potential source of systematic error in humid gas absorption studies. Thus, for the coupling losses of the resonators, one should consider an equation similar to Eq. (6),

$$P_{\text{coupling}} = P^{\text{dry}}_{\text{coupling}} + P^{\text{wet}}_{\text{coupling}}. \tag{8}$$

However, if the coupling film material, angle, and position of the film relative to the resonator mirrors are the same for both resonators of the module, then Eq. (7) is still valid.

D. Continuum measurements

It was decided to start the continuum absorption measurement at one fixed frequency near 130.38 GHz corresponding to the atmospheric window of transparency and at one fixed temperature of 40 °C. These limitations are not essential, but they allow saving time and effort at the development stage of the measurement method. The experiment started as usual from the spectrometer baseline record. Dry nitrogen evaporated from a liquid phase was slowly blown through the chamber until the humidity sensor [TESTO-645 (Ref. 26)] located near the center of the module indicated zero humidity and thermal equilibrium inside the chamber was achieved. During the baseline record, nitrogen was permanently blown through the chamber at atmospheric pressure. Then, a controlled amount of water vapor from a flask filled with double distilled liquid water was added stepwise to the nitrogen flow. Typical humidity in the chamber versus time of the experiment is shown in Fig. 7. Resonance widths in both cavities were measured at the end of each step after stable equilibrium conditions were achieved in the chamber. On attaining maximum desired humidity, the chamber was filled with dry nitrogen and the resonance widths were measured at low humidity. If the measured values coincided within experimental uncertainty with those measured at the beginning of the humidity cycle, then the experiment was considered to be successful. The gas mixture absorption coefficient inside the chamber was determined for each value of mixture humidity from the measured widths using Eq. (7). The results are presented in Fig. 8 by the filled circles. For comparison values of the absorption determined by each resonator of the module using Eq. (5) are also presented in Fig. 8. The empty circles and squares correspond to the short and long resonators, respectively. The solid curves in the figure are the second order polynomial functions fitted to the experimental points. All three curves differ significantly from each other. Thus, the figure demonstrates that in the conditions of the experiment, the wet gas absorption measurements systematic error may be comparable with the value of gas absorption if only one resonator is used for measurements.

To obtain a value of the continuum absorption from experimental data, one should allow for the contribution of discrete water vapor lines. It was calculated as a sum of Van Vleck–Weisskopf profiles of all intense lines up to 1 THz [the line list from MPM98 (Ref. 5)] using line strengths from HITRAN. For the line broadenings we used where possible experimental data[16,22,27] or results of complex Robert-Bonamy calculations by Gamache available from Ref. 28. After the contribution of discrete lines had been subtracted, the experimental data were fitted to the conventional empirical expression of the continuum absorption.[14] Under the described experimental conditions, the expression can be written as follows:

$$\alpha_{\text{cont}}(f,T) = \left[C_{\text{H}_2\text{O–N}_2} P_{\text{N}_2} \left(\frac{T_0}{T}\right)^{n_1} + C_{\text{H}_2\text{O–H}_2\text{O}} P_{\text{H}_2\text{O}} \left(\frac{T_0}{T}\right)^{n_2} \right] \left(\frac{T_0}{T}\right)^3 P_{\text{H}_2\text{O}} f^{n_3}, \tag{9}$$

where $C_{\text{H}_2\text{O–N}_2}$ and $C_{\text{H}_2\text{O–H}_2\text{O}}$ are, respectively, the coefficients related to water-nitrogen interactions and interactions among water molecules, P_{N_2} and $P_{\text{H}_2\text{O}}$ are the partial pressures of nitrogen and water vapor, T is the temperature (T_0 is usually equal to 300 K), $n_i (i=1,2)$ are the exponents of temperature dependences for the corresponding continuum com-

ponents, and n_3 is the exponent of the frequency dependence of the continuum usually[7–10,12,14] equal to two. It should be pointed out that by filling the module with dry nitrogen for determining resonator losses [Eq. (4)], we exclude from measurements the component of the so-called "dry" continuum, namely, the absorption related to nitrogen-nitrogen interaction having, under the described experimental conditions, a small but still quite measurable value[12] of about 2×10^{-8} cm^{-1}. This exclusion does not mean that the spectrometer described cannot measure dry nitrogen absorption (e.g., use of dry argon instead of nitrogen would do the job), but it eliminates the corresponding term in the total continuum absorption function, thus reducing the number of fitting parameters. Taking into account that the experiment was carried out at one frequency and at one temperature, formula (9) can be further simplified to the expression having only two fitting parameters corresponding to the desired continuum coefficients at the experimental temperature:

$$\alpha_{\text{cont}}(T) = [C^T_{\text{H}_2\text{O–N}_2} P_{\text{N}_2} + C^T_{\text{H}_2\text{O–H}_2\text{O}} P_{\text{H}_2\text{O}}] P_{\text{H}_2\text{O}} f^2. \quad (10)$$

The signal-to-noise ratio of the experimental data (Fig. 8) is obviously sufficient for determining both parameters.

Other coefficients of the empirical continuum absorption function (9) can be determined by analogy after carrying out similar experiments at different temperatures and throughout the frequency range of the spectrometer. Results of these experiments will be the subject of a separate publication.

As was mentioned earlier, the use of just one resonator for the water-related continuum measurements could introduce significant systematic error into the resulting absorption. It is interesting to analyze how strong the effect of humidity on the resonator parameters is. The proposed method allows determining only the total change in the resonator losses due to humidity ($P^{\text{wet}}_{\text{resonator}}$).

An equation for the change in loss caused by humidity for each of two resonators (assuming that the change is the same in both resonators) can be easily derived from Eqs. (1)–(4), (6), and (8) by analogy with Eq. (7) for the absorption coefficient,

$$P^{\text{wet}}_{\text{resonator}} = P^{\text{wet}}_{\text{reflection}} + P^{\text{wet}}_{\text{coupling}} = \frac{4\pi L}{c}[(\Delta f1 - \Delta f2) - (\Delta f1_0 - \Delta f2_0)]. \quad (11)$$

This loss related to humidity is presented in Fig. 9 as a function of humidity at different temperatures. It is worth noting that the dependence is linear within experimental uncertainty and has a strong dependence on temperature. At each temperature the linear dependence of the loss was observed at relative humidity ranging from 0% to 40%–60%, which is quite far from the dew point. Assuming a power dependence of the loss on temperature (similar to that commonly used for the continuum gas absorption parameterization), the following empirical function was fitted to the set of data obtained at temperatures ranging from −17 up to +60 °C:

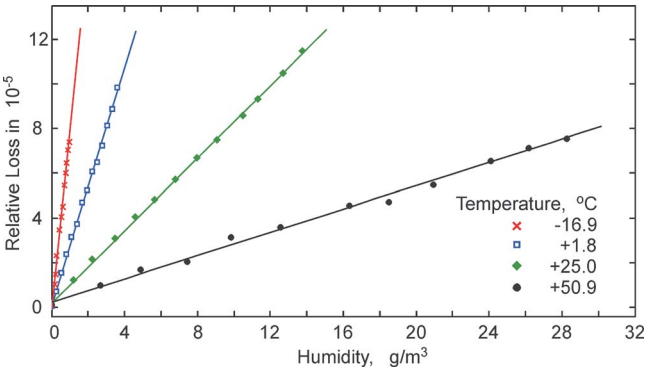

FIG. 9. (Color online) Experimentally determined relative additional resonator losses as a function of humidity (points) at different temperatures (shown in the figure). The solid lines are results of linear regression of the corresponding experimental points.

$$P^{\text{wet}}_{\text{resonator}}(T,\rho) = P_0 \rho \left(\frac{300}{T}\right)^N, \quad (12)$$

where ρ is absolute humidity in g/m^3, T is temperature, and P_0 and N are variable coefficients. The loss normalized to absolute humidity is shown in Fig. 10. The result of the fit is presented by the solid curve. The values $P_0 = 0.65(4) \times 10^{-5}$ (g/m^3)$^{-1}$ and $N = 16.5(4)$ were obtained from the fit.

At fixed temperature, absolute and relative gas humidities differ by a constant factor. Therefore, the resonator loss related to humidity plotted versus relative humidity also shows a linear dependence. However, the loss normalized to the relative humidity demonstrates a very different dependence on temperature. The dependence is plotted in Fig. 11. Within experimental accuracy the dependence can be considered to be linear.

IV. DISCUSSION

First of all let us consider accuracy of discrete line parameter measurements performed by the spectrometer described. As was discussed earlier, the statistical uncertainty is determined by the signal-to-noise ratio of the line record. For determination of possible systematic error a series of complementary experiments were performed[22,29,30] in which parameters of molecular spectral lines (in particular, pressure

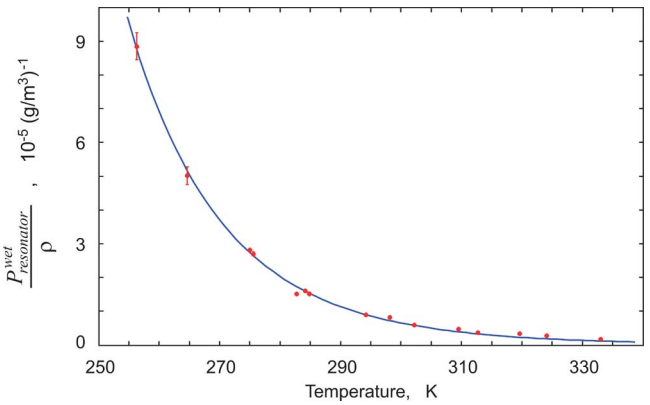

FIG. 10. (Color online) The relative resonator loss related to humidity, normalized to absolute humidity of the gas, vs temperature (empty circles). The solid line is a result of the power function [Eq. (12)] fit.

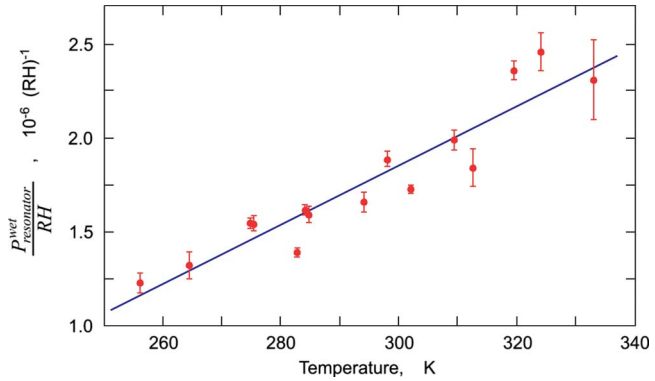

FIG. 11. (Color online) The same loss as in Fig. 10 normalized to relative humidity of the gas (empty circles). The solid line is a result of linear regression of experimental points.

broadening and shifting) measured by the resonator spectrometer were revised by a spectrometer of another type, namely, the spectrometer with radio-acoustic detection of absorption (RAD spectrometer),[31] the current version of which is described, e.g., in Ref. 32. Values of the parameters measured by the two spectrometers coincided within statistical uncertainty in all cases. As an example, results of the 118-GHz oxygen line self-pressure broadening studies by the RAD (Ref. 29) and resonator[18] spectrometers are presented in Fig. 12. The filled squares correspond to the line width experimentally measured by the RAD spectrometer. The same data were used in Fig. 3 in Ref. 29, where statistical uncertainties of these points (they are less than the size of the squares in Fig. 12) can be found. The measurement by the resonator spectrometer[18] is shown by an empty square. The solid line is the result of linear regression of the RAD spectrometer points. The dashed lines show the statistical uncertainty of the regression. Deviation of the resonator's point from the line can be seen in the inset of Fig. 12. It is really astonishing that the 300× extrapolation of the low-pressure measurement falls in such close vicinity to the result obtained by means of the resonator at atmospheric pressure. Such verification confirms reliability of the parameter value.

Another example is the pressure shift measurement of the 183-GHz water line center frequency. The shift in this line was experimentally determined for the first time from analysis of satellite data.[33] The value of the shift obtained in Ref. 33 varied by about a factor of two, depending on instrument and/or method of treatment. However, the authors

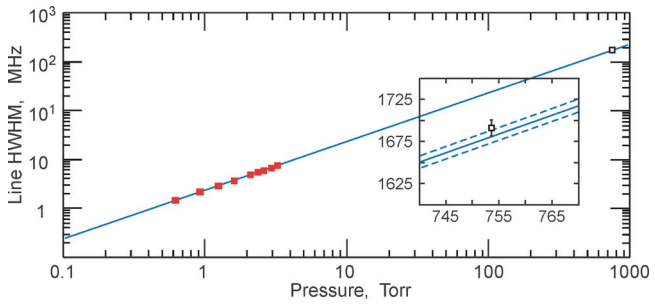

FIG. 12. (Color online) Self-pressure broadening of the 118-GHz oxygen line measured by RAD (filled squares) and resonator (empty square) spectrometers. See the text for details.

stated in their conclusions that "certain parameters, including the pressure shift, are hard to measure in the laboratory. MW limb-sounding instruments appear to be capable of providing a better measurement of the pressure shift of the 183-GHz water vapor line than any laboratory technique of which we are aware." Then the pressure shift in this line was measured by the two spectrometers mentioned above. The values of nitrogen and oxygen pressure shifts were, respectively, −91(24) and −84(30) kHz/Torr obtained by the resonator spectrometer[16] and −97(5) and −92(10) kHz/Torr by the RAD spectrometer.[30] Such coincidences of the parameters measured by fundamentally different spectrometers demonstrate that systematic error does not exceed the statistical one in both of them. The obtained data have the same sign and order of magnitude as the ones previously found from the satellite measurements[33] but have significantly better accuracy. It should also be mentioned that the result of the 183-GHz water line intensity measurement by the resonator spectrometer[16] coincided with the HITRAN database[34] value within 0.3%, which also proves minimization of systematic error sources in the spectrometer.

In the case of water-related continuum absorption measurements, manifestations of systematic error can be traced in Figs. 10 and 11. The spread of the experimental points in the figures exceeds their statistical uncertainty. The most probable reason for this systematic error is related to the temperature gradients of ~0.5 °C inside the chamber. The corresponding error of the gas humidity measurement varies within 1%–3% RH, depending on the average temperature in the chamber. The influence of this factor can be minimized by using a set of humidity sensors located around the module. Another possibility to exclude this factor is self-calibration of humidity inside the resonator by means of discrete water line profile recording and determination of the humidity (averaged over the whole volume of the resonator) from the line integrated intensity. Two other factors that may cause some systematic discrepancy may be hypothesized. Both of them, however, would not lead to the spread of points in Figs. 10 and 11. The first one is inaccuracy in coupling angles, leading, as shown above, to different humidity-related coupling losses in the resonators. To minimize this factor, in addition to careful alignment, the use of coupling films made of more hydrophobic materials (e.g., Teflon) may be recommended if such films are available. The second one is the identity of reflection loss changes in the concave and flat mirrors with a change in ambient gas humidity. The identity cannot be directly proven by experiment because it is impossible to maintain the same distribution of electromagnetic field in the cavity when the mirrors are interchanged. There seems to be no physical reason for such nonidentity; however, this factor cannot be excluded.

It follows from Fig. 8 that resonator loss related to humidity (hereinafter called "mirror effect" as the coupling loss contribution is much less than the reflection one) can constitute a large fraction of the total loss of the resonator filled with humid gas. However, the relative contribution of this loss is less if a longer resonator is used. Thus, hypothetic increasing of the resonator module length up to about 18 m (assuming that coupling, diffraction, and reflection losses as

well as sensitivity of the spectrometer are unchanged) and repeating the experiment under the conditions in Fig. 8 would make the absorption measured by each resonator and by the differential method indistinguishable because the systematic error due to the mirror effect would become less than the statistical error of the differential method.

Similar estimation can be made for the case of additionally heated mirrors like, e.g., in Ref. 14. The calculations (under assumptions that all additional humidity-related resonator losses are caused by mirrors and warm mirrors do not affect thermal equilibrium in the chamber) show that to reach coincidence of traces in Fig. 8, the mirrors should be about 95 K warmer than the surrounding humid gas.

It is also worth mentioning that the continuum measurement at elevated temperatures (e.g., 306–356 K as in Ref. 7) also helps to reduce the systematical error related to the mirror effect because in this case, relative contribution of the humidity-related resonator loss may also be made much smaller compared to the total loss of the resonator filled with humid gas. Using the continuum coefficients from Ref. 7, it can be found that the relative contribution of the mirror effect is less than 1% if the measurement temperature is above 360 K (5% at 333 K and 28% at 306 K). In Ref. 7 the coefficient of the term with squared water pressure of the total absorption (b' in the notation in Ref. 7) measured at 350.3 GHz in the experiment with pure water vapor was found to be 38% larger than the same coefficient measured in the experiment with humid nitrogen (b in the notation in Ref. 7). Similar differences were also observed in their other experiments. It was about 25% at 239 GHz and 10% at 213 GHz.[7] The authors presumably attributed the difference to "selective wall adsorption." However, the results of our experiments suggest that at least part of this difference is caused by adsorption of the water molecules onto the resonator mirrors. The frequency dependence of the difference observed in Ref. 7 can be naturally explained in this case because a thin water layer on a mirror surface should absorb more at shorter wavelengths. Quantitative estimation of possible systematic error of the absorption coefficients from Ref. 7 can be made under the assumptions that (i) the reflection loss in their spectrometer also linearly increased with gas humidity and (ii) the aforementioned 38% difference was caused by the mirror effect. With these assumptions, the effect would lead to overestimation of the b' coefficient in the pure water experiment, but it would not affect the b value in the humid nitrogen experiment. This speculation allows estimating the fraction of the total measured absorption in the humid nitrogen experiment, which was caused by the mirror effect to be $0.61 \times b \times P_{H_2O}^2$. Subtraction of this fraction from the term with linear water vapor pressure of the total absorption ($a \times P_{H_2O}$ in the notation in Ref. 7) and linear regression of the data gives a new value of a. Its temperature dependence can be found as described in Ref. 7. New values of a constant factor of $a(T)$ and its temperature exponent at 350.3 GHz are smaller than the values given in Ref. 7 by about 10%. This difference coincides by the order of magnitude with the above estimates of the mirror effect contribution at elevated temperatures.

The physical time limitations in the resonator spectrometer were assessed in Ref. 17. The time needed for scanning the whole BWO frequency range was estimated to be about 10 ms. In practice, a line record with sufficient signal-to-noise ratio takes more time. For example, for recording the 118-GHz oxygen line shown in Fig. 3, one would need (500 points per each resonance record at 1 μs per point scan speed, 128 back and forth scans, and 95 resonances) 12 s. Another 12 s would be necessary for the spectrometer baseline record. So, a high sensitivity record of atmospheric line profile can be done in a real time regime. The water-related continuum investigations take much more time, as can be seen from Fig. 7, because equilibrium conditions must be attained at each humidity point. One experimental cycle at a given temperature takes in practice about 1 working day, including chamber dehydration and this is usual for such measurements.[12]

As a general conclusion, the performed tests confirm that the spectrometer described in the present paper is a powerful tool for investigation of atmospheric absorption, including precise studies of spectroscopic parameters of broad discrete lines as well as studies of continuum absorption and, in particular, the most challenging water-related continuum. The proposed method permitted minimization of systematic error in both cases, making them less than the statistical one, at least in the case of the discrete line parameter measurements. Besides, the first adequate technique of eliminating systematic error caused by water molecule adsorption on resonator elements was proposed. The most important conclusion is that the achieved accuracy satisfies modern demands for atmospheric remote sensing data retrieval.

ACKNOWLEDGMENTS

The authors are grateful to Dr. P.W. Rosenkranz for his valuable comments on the manuscript. We also thank the unknown reviewer of the manuscript for his extensive work on improving readability of the paper. Studies described in this work were supported in part by the RFBR Grants (Grant Nos. 09-02-00053-a and 09-05-00586-a) and the Grant of the President of Russia (Grant No. MK-1163.2008.2).

[1] S. Payan, J. de La Noë, A. Hauchecorne, and C. Camy-Peyret, C. R. Phys. **6**, 825 (2005).
[2] L. S. Rothman, N. Jacquinet-Husson, C. Boulet, and A. M. Perrin, C. R. Phys. **6**, 897 (2005).
[3] A. Perrin, C. Puzzarini, J.-M. Colmont, C. Verdes, G. Wlodarczak, G. Cazzoli, S. Buehler, J.-M. Flaud, and J. Demaison, J. Atmos. Chem. **51**, 161 (2005).
[4] A. F. Krupnov, M. Y. Tretyakov, V. V. Parshin, V. N. Shanin, and S. E. Myasnikova, J. Mol. Spectrosc. **202**, 107 (2000).
[5] P. W. Rosenkranz, Radio Sci. **33**, 919 (1998); corrections in **34**, 1025 (1999).
[6] Q. Ma and R. H. Tipping, J. Quant. Spectrosc. Radiat. Transf. **82**, 517 (2003).
[7] T. Kuhn, A. Bauer, M. Godon, S. Buehler, and K. Kuenzi, J. Quant. Spectrosc. Radiat. Transf. **74**, 545 (2002).
[8] V. B. Podobedov, D. F. Plusquellic, and G. T. Fraser, J. Quant. Spectrosc. Radiat. Transf. **91**, 287 (2005).
[9] V. B. Podobedov, D. F. Plusquellic, K. E. Siegrist, G. T. Fraser, Q. Ma, and R. H. Tipping, J. Quant. Spectrosc. Radiat. Transf. **109**, 458 (2008).
[10] V. B. Podobedov, D. F. Plusquellic, K. M. Siegrist, G. T. Fraser, Q. Ma, R. H. Tipping, J. Mol. Spectrosc. **251**, 203 (2008).
[11] A. I. Meshkov and F. C. De Lucia, Rev. Sci. Instrum. **76**, 083103 (2005).
[12] A. I. Meshkov and F. C. De Lucia, J. Quant. Spectrosc. Radiat. Transf.

108, 256 (2007).
[13] M. Yu. Tretyakov, M. A. Koshelev, I. A. Koval, V. V. Parshin, Yu. A. Dryagin, L. M. Kukin, and L. I. Fedoseev, Atmos. Oceanic Opt. **20**, 89 (2007).
[14] H. J. Liebe, Int. J. Infrared Millim. Waves **5**, 207 (1984).
[15] C. Casto and F. C. De Lucia, Proceedings of the 63rd Ohio State International Symposium on Molecular Spectroscopy, 16–20 June 2008, Columbus, USA (http://molspect.mps.ohio-state.edu/symposium/Archive.html), p. 166.
[16] M. Yu. Tretyakov, V. V. Parshin, M. A. Koshelev, V. N. Shanin, S. E. Myasnikova, and A. F. Krupnov, J. Mol. Spectrosc. **218**, 239 (2003).
[17] M. Yu. Tretyakov, V. V. Parshin, M. A. Koshelev, A. P. Shkaev, and A. F. Krupnov, J. Mol. Spectrosc. **238**, 91 (2006).
[18] D. S. Makarov, I. A. Koval, M. A. Koshelev, V. V. Parshin, and M. Yu. Tretyakov, J. Mol. Spectrosc. **252**, 242 (2008).
[19] See: http://www.istok-mw.ru/ for brief information.
[20] R. I. Ovsyannikov and M. Yu. Tretyakov, J. Commun. Technol. Electron. **50**, 1400 (2005).
[21] P. W. Rosenkranz, IEEE Trans. Antennas Propag. **23**, 498 (1975).
[22] M. A. Koshelev, M. Yu. Tretyakov, G. Yu. Golubiatnikov, V. V. Parshin, V. N. Markov, and I. A. Koval, J. Mol. Spectrosc. **241**, 101 (2007).
[23] M. Yu. Tretyakov, M. A. Koshelev, V. V. Dorovskikh, D. S. Makarov, and P. W. Rosenkranz, J. Mol. Spectrosc. **231**, 1 (2005).
[24] M. Yu. Tretyakov, G. Yu. Golubiatnikov, V. V. Parshin, M. A. Koshelev, S. E. Myasnikova, A. F. Krupnov, and P. W. Rosenkranz, J. Mol. Spectrosc. **223**, 31 (2004).
[25] G. E. Dunaevsky and A. L. Inkhireev, Radioteh. Electron. (Moscow) **23**, 1987 (1988) (the journal is available in English translation as "Journal of Communications Technology and Electronics").
[26] See: http://www.testo.de for brief description.
[27] G. Yu. Golubiatnikov, M. A. Koshelev, and A. F. Krupnov, J. Quant. Spectrosc. Radiat. Transf. **109**, 1828 (2008).
[28] See: http://faculty.uml.edu/Robert_Gamache/ for data.
[29] G. Yu. Golubiatnikov, M. A. Koshelev, and A. F. Krupnov, J. Mol. Spectrosc. **222**, 191 (2003).
[30] G. Yu. Golubiatnikov, J. Mol. Spectrosc. **230**, 196 (2005).
[31] A. F. Krupnov, in *Modern Aspects of Microwave Spectroscopy*, edited by G. W. Chantry (Academic, London, 1979).
[32] A. F. Krupnov, G. Yu. Golubiatnikov, V. N. Markov, and D. A. Sergeev, J. Mol. Spectrosc. **215**, 309 (2002).
[33] H. C. Pumphrey and S. Bühler, J. Quant. Spectrosc. Radiat. Transf. **64**, 421 (2000).
[34] L. S. Rothman, D. Jacquemart, A. Barbe, D. C. Benner, M. Birk, L. R. Brown, M. R. Carleer, C. Chakerian, Jr., K. Chance, V. Dana, V. M. Devi, J.-M. Flaud, R. R. Gamache, A. Goldman, J.-M. Hartmann, K. W. Jucks, A. G. Maki, J.-Y. Mandin, S. T. Massie, J. Orphal, A. Perrin, C. P. Rinsland, M. A. H. Smith, J. Tennyson, R. N. Tolchenov, R. A. Toth, J. Vander Auwera, P. Varanasi, and G. Wagner, J. Quant. Spectrosc. Radiat. Transf. **96**, 139 (2005).